Analysis of rigid and semi-rigid steel-concrete composite joints under monotonic loading
Part I: Finite element modelling and validation

C. Amadio† and M. Fragiacomo‡

Department of Civil Engineering, University of Trieste, Piazzale Europa 1, 34127 Trieste, Italy

Abstract.   The paper concerns the modelling of rigid and semi-rigid steel-concrete composite joints under monotonic loading through use of the Abaqus program, a widespread finite element code. By comparing numerical and experimental results obtained on cruciform tests, it is shown that the proposed modelling allows a good fit of the global joint response in terms of moment-rotation law. Even the local response in terms of stresses and strains is adequately predicted. Hence, this numerical approach may represent a useful tool for attaining a better understanding of experimental results. It may also be used to perform parametric analyses and to calibrate simplified mechanical models for practical applications.

Key words: Abaqus code; beam-to-column connection; finite element modelling; non-linear analysis; semi-rigid joints; steel-concrete composite joints.

1. Introduction

The use of braced steel-concrete composite frames has many advantages with respect to traditional non-composite structures, such as less overall weight compared to concrete structures and larger stiffness compared to steel structures. A further benefit is the possibility to obtain a degree of structural continuity between contiguous spans by placing adequate reinforcement in the slab. This can be achieved easily and with little additional cost. A modern trend in order to reduce labour cost, which is a crucial aspect of the total building cost, is to simplify as much as possible the steel beam-to-column connection, thus obtaining semi-rigid joints.

In spite of the many benefits of this modern construction technique, the semi-rigid steel-concrete composite frame has yet to be extensively employed. The main reason for this is difficulties in adequately predicting the joint behaviour, while another important factor is the lack of validated design methods. Recently, however, important steps forward have been made for both the prediction of joint behaviour (Leon 1990, Eurocode 4 1992, 1997, Filippou and Zulfiqar 1992, Tschemmernegg and Queiroz 1995, Nethercot 1998, Tschemmernegg *et al.* 1998, Fang *et al.* 1999, etc.) and the determination of simplified design criteria (Nethercot 1995a, 1995b, Leon *et al.* 1996, Li *et al.* 1996d, Wong *et al.* 1996, Leon 1998, Leon and Darwin 1998).

---

†Associate Professor
‡Research Engineer

The moment-rotation law of a semi-rigid composite joint is difficult to predict because of the many parameters that affect the behaviour. The most important parameters are:

1) *the internal forces that develop in the slab*, which depend on the type of slab (solid, cast in situ, pre-cast, cast on steel sheeting), the characteristics of reinforcement, the ratio between geometrical dimensions of the slab and steel beam, the concrete tensile strength;

2) *the beam-to-column and beam-to-beam interaction* and, therefore, the type of connection between steel beam and column, the method of construction of the slab in the zone around the column (in contact with the column or completely detached), the type of construction of the composite beam (propped or unpropped), and the type of connection between steel beam and slab (full or partial);

3) *the type of beam, column and details* and, therefore, the class of steel beam, the quality of steel, the type of column (steel, encased, or concrete filled hollow sections), and the presence of stiffeners on the column web;

4) *the type of load* and, therefore, the distribution along the beams and the structure, and the manner of application (monotonic symmetric or non-symmetric, cyclic, static, dynamic).

Since the number of parameters affecting the composite joint is considerable, it is evident that an exhaustive experimental study would be too complex and expensive to be performed. However, knowledge of the real moment-rotation law for the joint or, at least, a good approximation of this quantity is needed for a correct design of the composite frame and, thereby, to facilitate its widespread use. Four different approaches can be employed for both steel (Nethercot and Zandonini 1989, Mazzolani and Piluso 1996) and composite (Zandonini 1989) semi-rigid joints:

1) e*xperimental*, in order to investigate the most important mechanisms of the joint;

2) *numerical*, in order to understand the experimental mechanisms and to check more extensively the validity of simplified models proposed for practical design. This approach is generally based on use of the finite element technique;

3) *mechanical* (or *per component*), where the joint is schematised through a number of springs ("components") arranged in such a way as to approximate the real behaviour;

4) *analytical*, where the moment-rotation law is defined through analytical laws.

Both mechanical and analytical approaches are based on a simplified plane analysis. The goal of these approaches is to make the joint modelling straightforward and easily employable by the designer.

Many efforts have been made so far on both mechanical (Anderson and Najafi 1994, Tschemmernegg and Queiroz 1995, Ren *et al*. 1996, Dissanayake *et al*. 2000, Kattner and Crisinel 2000, Faella *et al*. 2000, etc.) and analytical (Nethercot and Zandonini 1989, Li *et al*. 1996b, Xiao *et al*. 1996, Faella *et al*. 2000, etc.) approaches. Several tests have also been performed (Benussi *et al*. 1989, 1995, Puhali *et al*. 1990, Anderson and Najafi 1994, Xiao *et al*. 1994, Li *et al*. 1996a, Li *et al*. 1996c, Ren *et al*. 1996, Leon *et al*. 1998, Cruz *et al*. 1998, etc.). Conversely, only few works have investigated the numerical modelling of the composite joint by using a two- (Bursi and Ballerini 1997, Bursi and Gramola 1997) or a three-dimensional finite element modelling (Amadio and Piva 1995), unlike the steel semi-rigid joint, for which several two- and three-dimensional finite element approaches have been proposed (Nethercot and Zandonini 1989).

With an aim to at least partially fill this gap, this paper presents the results of some analyses performed on rigid and semi-rigid steel-concrete composite joints using the Abaqus code (Hibbit *et al*. 1997), a widespread finite element program. The proposed numerical approach is based on a 3D modelling of the concrete slab, steel column and steel beam. The contact between slab and column, the interaction between slab and beam (through the head studs) and the beam-to-column connection (through bolting and flanges) are adequately considered. The numerical results fit well with the experimental ones

obtained on symmetrical cruciform specimens in terms of both global and local behaviour.

This approach permits a thorough understanding of the most important phenomena affecting the joint behaviour and, therefore, can be used to investigate the complex interaction phenomena among the different components of the joint. Furthermore, this approach may be employed to perform parametric analyses and to control the accuracy of simplified mechanical prediction models. Conversely, because of the large computational demand, it is not suitable for practical design of composite frames. To this purpose, the mechanical approach, and particularly the component method, is the best way to obtain adequate results without large computational effort.

2. Modelling of semi-rigid composite connections

Before describing the analyses performed, it is useful to illustrate how the materials that constitute the joints have been modelled using the Abaqus code.

2.1. Modelling of steel beam and column

The steel beam and column have been schematised by using S8R shell elements, an eight-node shell element with five degrees of freedom per node and reduced integration. This type of element has been chosen because of its computational efficiency, even in a non-linear plastic analysis. More accurate solutions can be obtained with respect to the four-node shell elements using the same number of degree-of-freedoms. The choice of mesh has been made for each case of study in such a way as to obtain stable solutions. As such, meshes that are denser in the connection zone and wider elsewhere have been selected (Figs. 5 and 13).

The steel has been modelled using a three-linear stress-strain law, symmetric in tension and compression, characterised by an elastic-plastic with hardening behaviour and yielding plateau beyond the elastic phase. According to the experimental behaviour, the plastic strain at the end of the yielding plateau ε_h and the modulus in hardening phase E_h have been evaluated as:

$$\varepsilon_h = 15\varepsilon_y \tag{1}$$

$$E_h = 0.015E \tag{2}$$

where ε_y and E are, respectively, the yield strain and Young's modulus of steel.

2.2. Modelling of reinforced concrete slab

The reinforced concrete slab has also been schematised using the S8R shell element. All complex phenomena of interaction with beam, columns, and head stud connectors may be correctly evaluated in this way. Unlike one-dimensional modelling, both shear flexibility and biaxial stress state affecting some parts of the slab can be considered. Compared to a two-dimensional modelling (Bursi and Ballerini 1997, Bursi and Gramola 1997), the stress distribution in the slab, including the shear-lag effect, can be better evaluated. The interaction with head stud connectors and the column can also be adequately represented. Since the slab plays a fundamental role in the behaviour of the composite joint, accurate modelling of concrete in the tensile zone, including the tension stiffening effect, is a primary
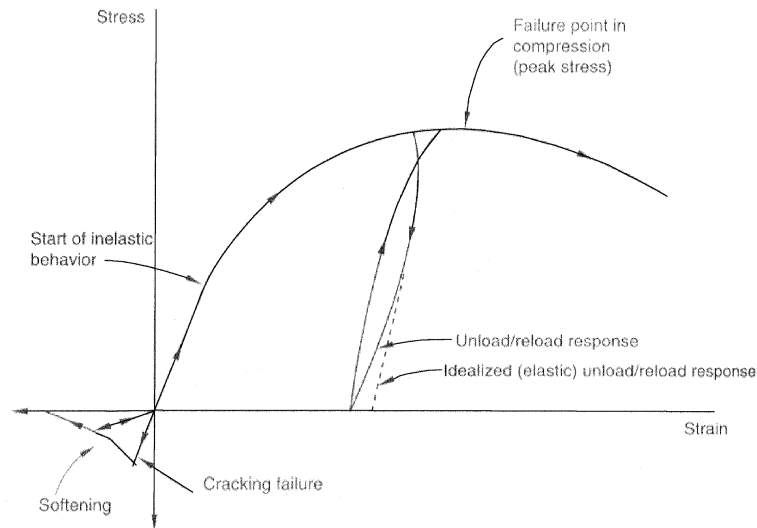
Fig. 1 Uniaxial stress-strain law adopted by Abaqus for concrete

element to achieve a good outcome in the numerical analysis.

The problem of cracking can be dealt with in two different ways in finite element simulations of reinforced concrete elements. Reinforcing bars and concrete can be modelled as two different elements, by adequately characterising the interaction along the boundary of these materials (Chen 1984, CEB 1997, Manfredi *et al.* 1999). Another possibility is to smear the reinforcement in the concrete element, by also considering the properties of the cracked material as diffused into the element volume (Crisfield 1991, Bažant and Jirásek 2002). Abaqus adopts the second approach, which is referred to as "smeared cracking". The effects due to the interaction between concrete and bars in tensile zones, such as bond, dowel effect and mechanisms occurring in the cracked phase, cannot be separately considered in this approach. Conversely, the load transfer in the cracked phase between concrete and steel bars can be described in a global way by using a fictitious softening law.

The uniaxial compressive and tensile stress-strain laws of concrete adopted by Abaqus are plotted in Fig. 1. The concrete is considered in compression as a linear-elastic material until the stress reaches a value equal to 40% of the ultimate strength f_c. Beyond this limit, because of the plastic strains, a non-linear curve is followed up to failure. A subsequent softening branch, calibrated on the basis of the confinement pressure, can be considered as well. In this paper, Saenz's law proposed by the CEB-FIP Model Code 90 (1993) has been used, with the further simplification of a perfectly plastic branch without softening beyond the peak compressive strength up to the ultimate strain ε_{cu}.

In the Abaqus code, cracking is considered as occurred when the stress in a generic point reaches a collapse surface known as the "crack detection" surface (Fig. 2). According to this approach, therefore, the cracking phenomenon does not represent a crack opening in a point, but rather it is a variation of stiffness and stress in the integration points where the critical value has been achieved. The behaviour of concrete in the post-cracked phase is described through a softening law (Fig. 1). This law must be able to represent the tensile behaviour of reinforced concrete structures, including the tension stiffening effect, while at the same time providing a good guarantee of numerical convergence. Numerous problems are still unresolved regarding above all the evaluation of a suitable softening law. In this paper, the
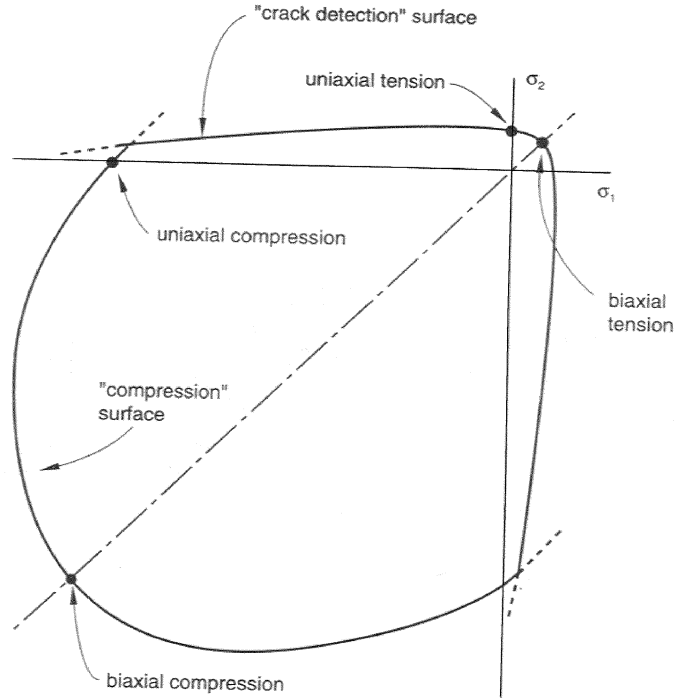
Fig. 2 Biaxial strength domain in the principal stress plain adopted by Abaqus for concrete

Stevens *et al.* law (1991) is employed. According to this softening model, the medium tensile force in concrete does not vanish when the reinforcement yields. This law was demonstrated to provide good results for modelling the concrete slab of a composite beam (Amadio and Altin 1995).

Longitudinal and transversal reinforcement placed in the slab at two possible levels are represented by four layers. For reinforcement, a three-linear stress-strain law similar to that adopted for the steel beam and column has been employed. In this case, according to the different experimental behaviour of such a type of steel, the following values have been assumed:

$$\varepsilon_h = 3\varepsilon_y \tag{3}$$

$$E_h = 0.020E \tag{4}$$

The approach adopted by Abaqus for modelling reinforced concrete slabs, despite some convergence problems due to the softening law, is practically the only one employable for a three-dimensional analysis.

2.3. Modelling of shear studs

Shear stud connectors have been modelled by non-linear springs located at the beam-to-slab interface in the real position. Each spring is connected to the concrete slab and steel beam through rigid links. The adopted constitutive law was proposed by Aribert (1995):

$$Q = Q_u(1 - e^{-C_1|\gamma|})^{C_2} \tag{5}$$

where Q, Q_u are the current and ultimate shear strength, respectively, γ is the relative slip between steel beam and concrete slab, and C_1, C_2 are two constants depending on the geometry of stud (height and diameter), spacing and concrete properties. In these analyses, the values $Q_u = 130$ kN, $C_1 = 0.7$ mm^{-1} and $C_2 = 0.8$ have been assumed for 12 mm diameter head studs, along with an ultimate slip $\gamma_u = 6$ mm.

2.4. Modelling of bolts

An appropriate modelling of the bolts connecting the steel beam and column is necessary for a correct representation of the joint behaviour. The preloading of bolts and possible detaching between the endplate and column flange during the load process are in particular very important. The preloading of bolts causes contact between the whole endplate and the column flange. When the hogging bending moment in the joint increases, the upper part of the endplate detaches and only the lower part maintains contact with the column flange. In order to avoid stress peaks and to account for the presence of the nuts, each bolt has been modelled through five non-linear beam elements parallel to the bolt axis connecting the column flange and the endplate meshes. One beam element has been arranged in the centre of the shank. The other four beams have been placed, equally spaced, near the lateral surface of the shank on the vertices of a cross. For 20 mm diameter bolts, each beam is 12 mm from the shank centre. The area of the shank has been divided in the same parts among each beam element. The preloading of bolts has been applied by two compressive forces applied at the ends of each beam. The stress-strain law for steel of bolt is bilinear without a yielding plateau, with the same modulus in the hardening phase E_h as that adopted for reinforcement (Eq. 4).

2.5. Application of boundary conditions and loading procedure

Modelling of the contact zone between the endplate and column flange must take into account possible detachment. This is achieved by linking the nodes of the two meshes through beam elements characterised by elastic behaviour and large axial stiffness. When the load increases, in some of the contact elements the stress decreases, and an inversion of stress may occur. If the stress turns from compression to tension, the contact element is removed according to a step-by-step updating procedure provided for by Abaqus. In this way, the convergence problems due to the use of non-linear contact elements between two nodes, such as unidirectional gaps or non-linear axial springs, are overcome. The contact between concrete slab and column has been modelled likewise using rigid links. The stress is assessed at each load step for every link, which is removed if the stress turns to tension and detachment occurs.

The numerical results have been obtained through a non-linear analysis performed by neglecting the second order effects. The arc-length method (Crisfield 1991), which can be used to follow possible decreasing load-displacement and stress-strain branches, has been employed as a convergence algorithm. Boundary conditions and bolt preloading have been imposed in the first load step, as well as the equality of vertical displacements of the concrete slab and steel beam. In the following load steps, the external load has been augmented according to the experimental procedure. The increment of load multiplier is automatically computed by the Abaqus program. The stresses in all contact elements (beams and rigid links) are assessed at the end of each load step. A restart of the analysis with removal of the contact elements in tension is performed in the case of detachment between the endplate and the column flange or the concrete slab and column.

3. Numerical-experimental comparisons

In order to validate the proposed finite element schematisation, a comparison between numerical and experimental results is presented for different types of composite joints. The experimental results refer to the tests performed at the University of Trieste on cruciform specimens, which were symmetrically and monotonically loaded up to collapse (Fig. 3). Both rigid and semi-rigid joints were tested (Benussi *et al.* 1989, Puhali *et al.* 1990). The details and geometric properties of the specimens are summarized in Tables 1 and 2. The mechanical properties of concrete and steel used in the specimens are reported in Tables 3 and 4, respectively.
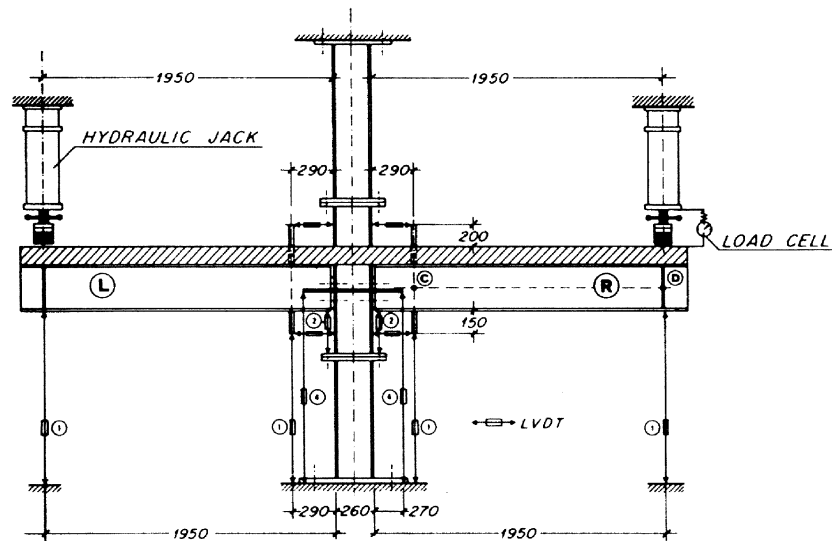

Fig. 3 Test set-up (Puhali *et al.* 1990)

Table 1 Specimen details

Specimen	Joint type	Beam-to-column connection	Web stiffening by horizontal steel plates	Top and bottom reinforcement
RJ14	Rigid	Welded	Both bottom and top flange beam	8 No. 14 mm ϕ
SJA14/2	Semi-rigid	Partial depth endplate	None	+ 8 No. 6 mm ϕ
SJA14	Semi-rigid	Partial depth endplate	Only bottom flange beam	8 No. 14 mm ϕ
SJB14	Semi-rigid	Flush endplate	Only bottom flange beam	+ 8 No. 6 mm ϕ
SJA10	Semi-rigid	Partial depth endplate	Only bottom flange beam	8 No. 10 mm ϕ
SJB10	Semi-rigid	Flush endplate	Only bottom flange beam	+ 8 No. 6 mm ϕ

Table 2 Geometric properties of the specimens (measures in mm)

Beam profile	Column profile	Concrete slab	Transversal reinforcement	Beam-to-slab connection
IPE300	HEB260	1000×120	Stirrups 1 No. 6 mm ϕ @ 250 mm c/c	Head studs 2 No. 12 mm ϕ @185 mm c/c

Table 3 Mechanical properties of the concrete used in the specimens

Medium compressive cylindrical strength f_{cm} (N/mm^2)			Medium tensile cylindrical strength f_{ctm} (N/mm^2)			Ultimate strain ε_{cu} (%)	Medium elastic modulus E_{cm} (N/mm^2)		
RJ14	SJA14/2	Others	RJ14	SJA14/2	Others	All specimens	RJ14	SJA14/2	Others
23.7	31.4	34.8	3.3	3.7	3.3	0.3	30000	32330	33240

Table 4 Mechanical properties of the steel used in the specimens

Type of steel	Yield stress f_y (N/mm^2)			Tensile strength f_u, f_t (N/mm^2)			Ultimate strain ε_u (%)			Elastic modulus E (N/mm^2)
	RJ14	SJA14/2	Others	RJ14	SJA14/2	Others	RJ14	SJA14/2	Others	All specimens
IPE 300	324	338	288	450	386	430	28.7	36.2	28	206000
HEB 260	325	335	325	479	487	479	28.7	31.2	28	206000
14 mm bars	427	428	413	667	663	612	27.1	27.1	17	206000
10 mm bars	-	-	495	-	-	695	-	-	20	206000
6 mm bars	384	393	464	533	538	658	30	30	22	206000
20 mm bolts	-	640	640	-	800	800	-	12	12	206000

3.1. RJ14 rigid joint

The first specimen analysed in this paper, tested by Puhali *et al.* (1990), is a rigid joint denoted as RJ14 by the authors. In this joint, the beam-to-column connection is welded. The web column is stiffened by horizontal steel plates welded at the level of the bottom and top beam flanges (Fig. 4a). The longitudinal reinforcement in the slab is given by eight 14 mm diameter bars at the top and eight 6 mm diameter bars at the bottom, which correspond to a medium (1.21%) reinforcement percentage. The shear connection between the concrete slab and steel beam is full according to Eurocode 4 (CEN 1992), with limited relative slips. During the test, the strains of the top reinforcing bars were monitored by 12 electric strain gauges applied in three cross-sections X, Y, and Z (Fig. 4b).
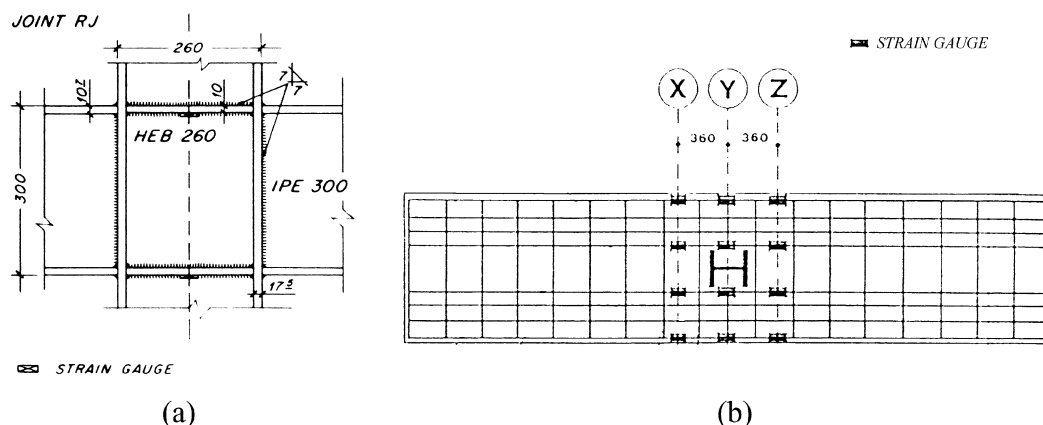

(a)									(b)

Fig. 4 Detail of the steel beam-to-column connection (a) and of the reinforcement in the concrete slab (b) for the RJ14 joint
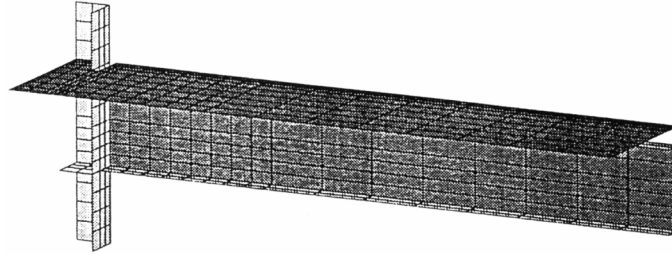
Fig. 5 Mesh adopted for modelling the test performed on the RJ14 joint
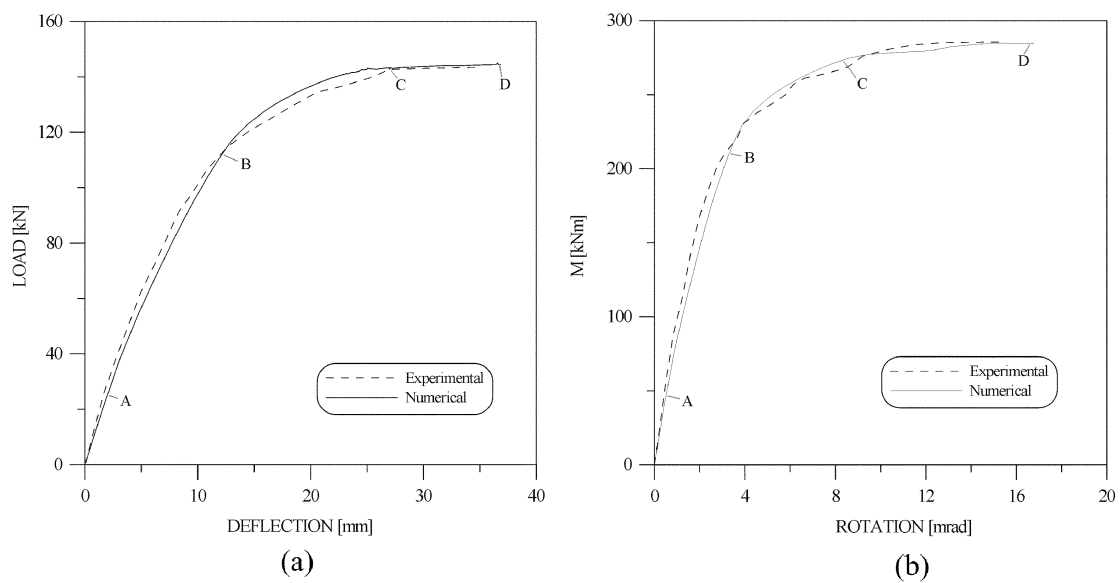

Fig. 6 Comparison between experimental and numerical results for the RJ14 joint in terms of load vs. vertical displacement (a) and moment vs. rotation (b) curves

For the symmetry, only a quarter of the structure has been considered in the finite element schematisation. The adopted mesh, which is quite dense (420 elements), is displayed in Fig. 5. A comparison with the experimental response is plotted in Fig. 6 in terms of load vs. deflection and moment vs. rotation curves. The deflection is evaluated at the end of the composite cantilever and the bending moment on the external surface of the column flange. The rotation is calculated in the cross-section of the beam 290 mm from the column flange, the same location where it was measured during the test. The letters A to D refer to the beginning of cracking, yielding of steel beam, yielding of reinforcement, and collapse of the joint. Numerical and experimental values match well, as can be observed from Table 5.

As confirmed by almost all experimental tests performed thus far, the beginning of cracking in the concrete slab occurs when the bending moment is about 20 to 25% of the collapse value. The first cracks generally occur near the column flanges, and subsequently spread toward the external sides of the slab, in a direction nearly perpendicular to the beam axis. After the beginning of cracking, the moment-rotation law is still nearly linear, with stiffness slightly smaller than in the non-cracked phase. The stiffness variation due to cracking is gradual in the numerical curve. The adopted softening law

Table 5 Comparison between experimental and numerical moments for the RJ14 joint

Values	Point A: first cracking	Point B: yielding of the beam	Point C: yielding of the bars (X sect.)	Point D: collapse of the joint
Experimental	47 (kNm)	213 (kNm)	263 (kNm)	290 (kNm)
Numerical	47 (kNm)	216 (kNm)	269 (kNm)	292 (kNm)

considers an unloading of the concrete and a non-instantaneous transfer of internal force to the reinforcement. Beyond the first cracking, the joint behaviour is mostly influenced by:

- yielding of the steel elements (steel profile and reinforcement);
- slips between steel beam and concrete slab;
- shear stress redistribution in the slab;
- interaction between the slab and column in the contact zone.

The plastic phase generally occurs at about 75 to 90% of the collapse load, and implies a large yielding of both reinforcement and steel profile, respectively, in tension and compression.

Two diagrams describing the trend of relative slip between the slab and steel beam with the external load near to the column and at the end of the cantilever beam, respectively, are plotted in Fig. 7. The numerical modelling fits quite well with the experimental results, despite that the prediction of this local response is rather complex. The experimental result monitored by linear voltage displacement transducers (LVDTs) placed near to the column is characterised by a first phase when a positive slip between the steel beam and the concrete slab occurs. Afterwards, an inversion of the phenomenon due to cracking of the slab and yielding of the reinforcement may be noted. The slab elongation becomes larger than the beam deformation and the slip becomes negative. The phenomenon is numerically quite
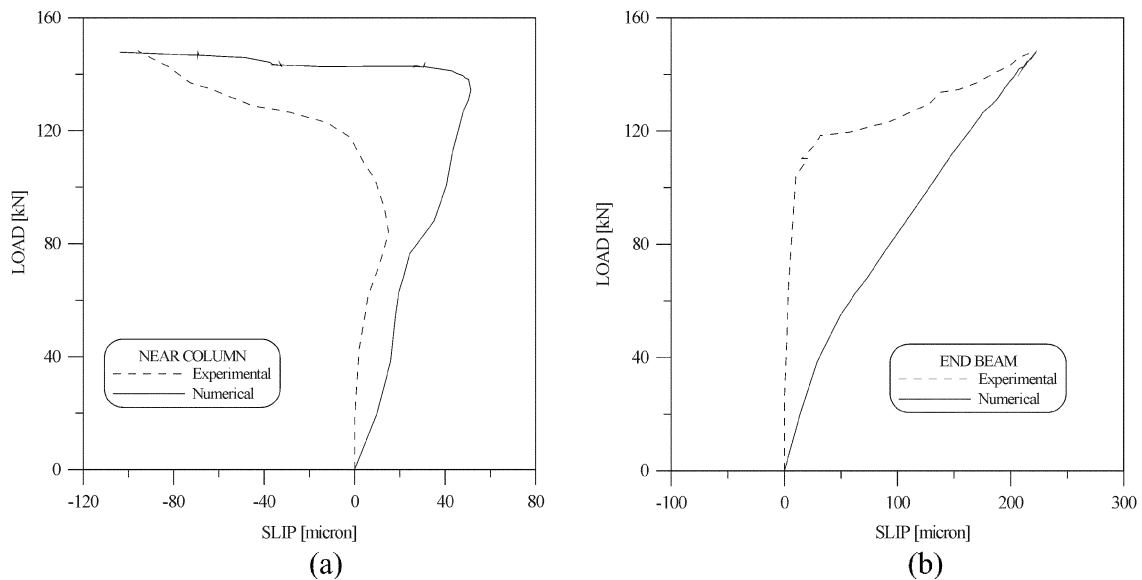

Fig. 7 Comparison between experimental and numerical results for the RJ14 joint in terms of load vs. slip curve near the column (a) and at the end of the cantilever beam (b)
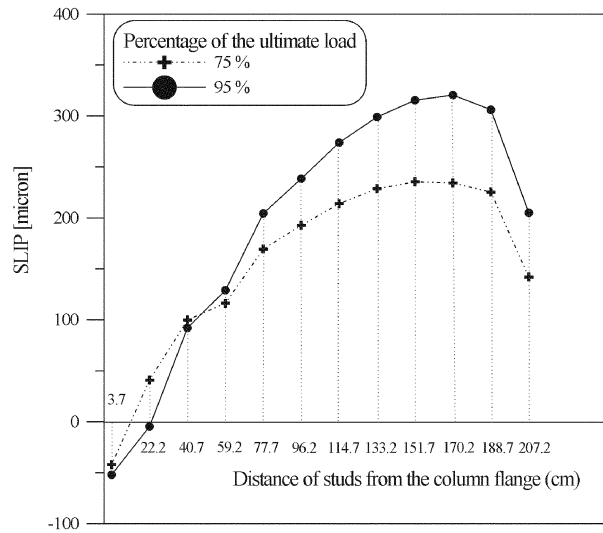
Fig. 8 Slip distribution along the beam axis for the RJ14 joint at different values of load

well fitted, even though the natural bond existing between the steel beam and concrete slab, which affects the response in the initial phase, has not been modelled. Conversely, the absence of slip inversion is noted at the free end of the beam, and the numerical curve is more gradual with respect to the experimental one. In such a case the influence of the bond, also due to the concentrated load, is more important and noticeable slip occurs only after cracking and yielding of reinforcement.

Some important observations are made concerning the slip distribution along the beam axis obtained using the numerical modelling (Fig. 8). The experimental data are not available along the whole beam axis, but only near the column and at the end of the cantilever beam (Fig. 7). The slip distribution is affected by several phenomena, usually neglected in one- and two-dimensional modelling, such as the shear lag effect, cracking of the concrete slab and the interactions among the column, slab and connection system. On the basis of the performed analysis, the first stud near to the column is almost unloaded during the whole loading history and its deformed shape is opposite to the other connectors even near the collapse (95% of the ultimate load). The other studs show a slip increasing toward the middle and decreasing toward the end of the cantilever beam. This trend is more prominent for large loads, when the studs near the end of the cantilever beam are less stressed compared to those in the middle of the span, because of the minor confinement action provided by the concrete slab.

Another important comparison in terms of local quantities is provided in Fig. 9, which presents the load vs. strain curves for the external and internal reinforcing bars in the X cross-section (see Fig. 4). Again, the numerical results fit well with the experimental ones. However, in the numerical responses, the transition between non-cracked and cracked phases is not as prominent as in the experimental test. Similar results were obtained for the other bars and cross-sections. Some comparisons have also been carried out for the strains monitored in horizontal steel plates that stiffen the column web. The outcomes confirm the possibility to also accurately predict these local quantities.

A comparison between the cracking pattern monitored in the test and the strain distribution obtained by using the proposed modelling is reported in Fig. 10. Three values of external load are considered: 22 kN (beginning of cracking in the slab), 58 kN (well-cracked slab), and 120 kN (yielded steel beam). The darker zone represents the part of the slab that is not yet cracked. The zone with a slightly brighter
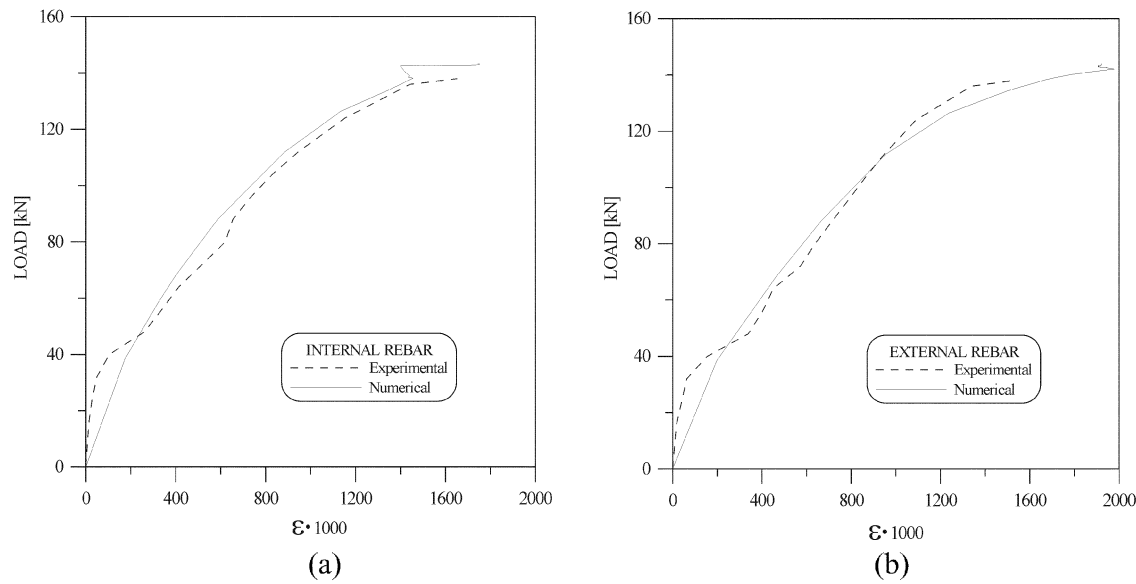
Fig. 9 Comparison between experimental and numerical results for the RJ14 joint in terms of load vs. strain curve for internal (a) and external (b) reinforcing bars in the X section
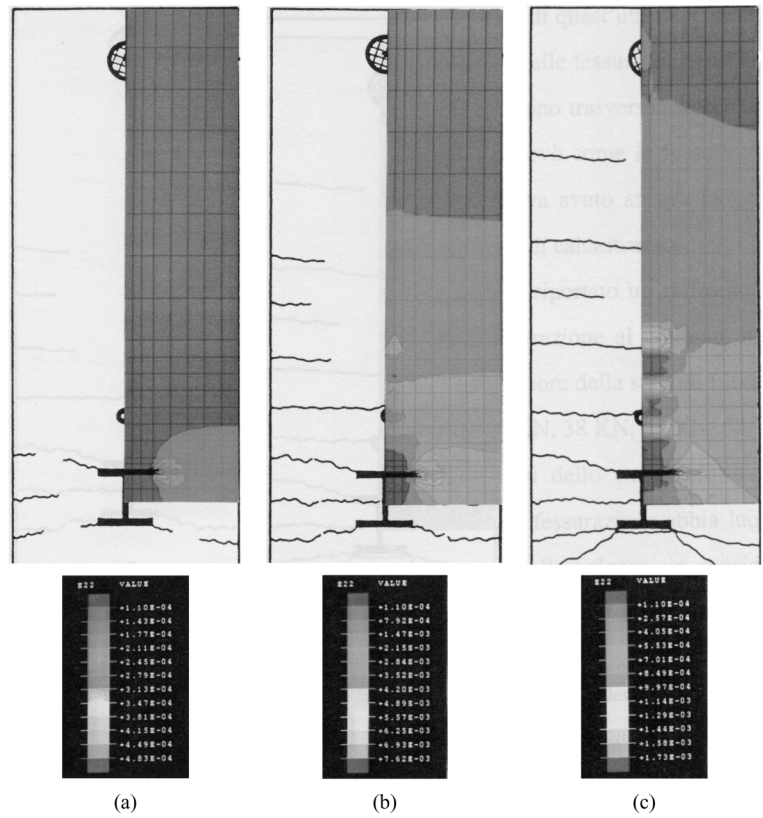

Fig. 10 Comparison between pattern of recorded cracks and numerical strain distribution for the RJ14 joint under a load of 22 kN (a), 58 kN (b) and 120 kN (c) (dark zones: less strained; bright zones: more strained)
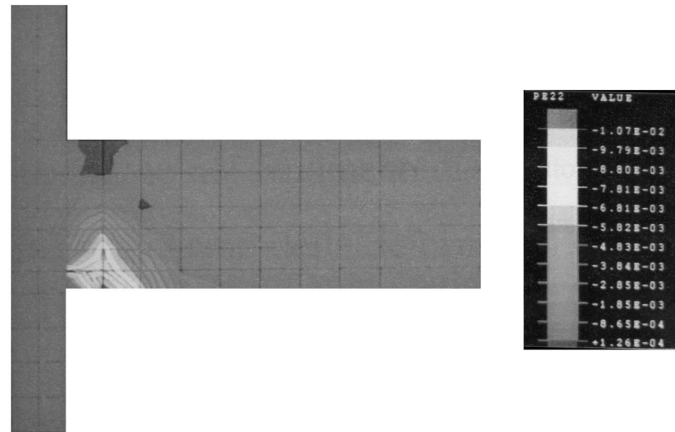
Fig. 11 Distribution of plastic strains in the column and steel beam for the RJ14 joint under the collapse load (dark zones: tensile strains; bright zones: compressive strains)

colour gradation represents the part that has just overcome the "crack detection" surface (Fig. 2). Such a zone is characterised by the absence of cracks that are visible to the naked eye, but with the presence of micro-cracks that are continuously spread into the volume. The zones indicated by gradually increasing brightness represent the parts that are gradually more strained. Again, the numerical results fit well with the experimental ones. The alternate zones along the beam axis of dark and bright colour gradations represent non-cracked and cracked zones due to the presence of connection studs.

In addition to the analysis of the experimental results, the proposed finite element modelling provides further possibilities to investigate the behaviour of the composite joint. For example, in Fig. 11, the distribution of plastic strains into the steel beam and column is displayed under the collapse load (point D in Fig. 6a, $P = 150$ kN). It may be noted that only the beam is plasticized. The plastic strains occur first in the lower part of the web and in the bottom flange of the beam, and afterwards spread upward. At collapse, the upper part of the beam has also plasticized. Conversely, no plastic strain can be noted in the column, because of the web stiffening by horizontal steel plates. These plates prevent the column web from plasticization and local buckling phenomena, and increase the stiffness of the composite joint.

On the basis of the numerical analysis it has also been observed that an increase in load augments, most of all, the stresses in the bottom flange of the beam, which yields for compression near the collapse load. The tensile zone is bounded to a small area near the top flange of the beam because of the important role played by the reinforcement in the slab, which carries most of the tensile force and raises the neutral axis in the plastic phase.

3.2. SJA14/2 semi-rigid joint

The second specimen analysed in this paper is a semi-rigid joint denoted as SJA14/2 by Puhali *et al.* (1990), the steel beam-to-column connection of which is represented in Fig. 12. It differs from the rigid joint RJ14 in the absence of column web stiffening and in the simplicity of the steel beam-to-column connection, which is realised through a partial depth endplate welded to the beam and bolted to the column flanges. Four high-strength 20 mm diameter bolts grade 8.8 according to Eurocode 3 (CEN 1992) were used. All other details are the same as those of the RJ14 rigid joint. Compared to RJ14, a more dense mesh of 680 shell elements has been adopted in order to obtain accurate solutions (Fig. 13).
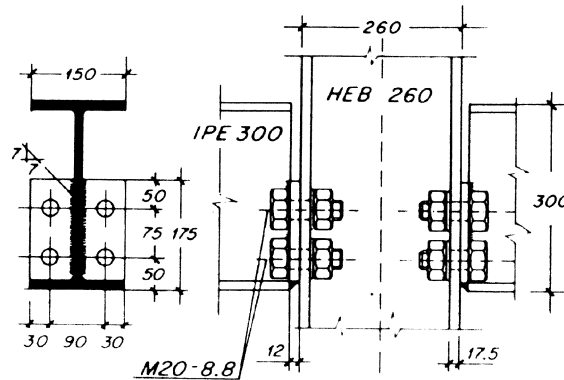
Fig. 12 Detail of the steel beam-to-column connection for the SJA14/2 joints
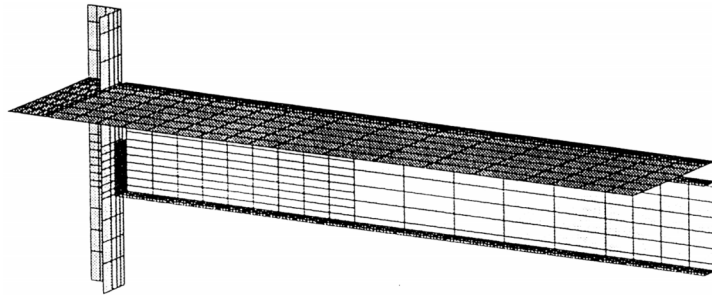

Fig. 13 Mesh adopted for modelling the test performed on the SJA14/2 joint

Careful consideration has been used in modelling the beam-to-column connection and the part of the beam web close to the column. The fillets of the beam and column profiles have been modelled as well, using shell elements of appropriate height and thickness.

A comparison between the numerical and experimental response is plotted in Fig. 14 in terms of the moment vs. rotation curve. The global response of the joint is adequately evaluated; however the numerical solution does not allow determination of the available ductility, because of convergence problems. The experimental test, therefore, in this case represents an indispensable tool for a full validation of the numerical response. The letters A to D refer to the beginning of cracking in the slab, yielding of the steel column, yielding of reinforcement (at the X cross-section), and yielding of the steel beam. Numerical and experimental values are very close, as can be observed in Table 6. In this case, the absence of column web stiffening produces an early yielding of the column and a significant reduction of the joint stiffness in the cracked phase. The collapse occurs without full yielding of the steel beam.

The load vs. slip curves near the column flange and at the end of the cantilever beam are quite similar to those already discussed for the rigid joint RJ14. The main difference concerns the value of the load for which the slip turns from positive to negative values; the value is lower in this case.

Fig. 15 displays the stress distribution in the column and steel beam for a moment in the joint of 223 kNm, equal to 95% of the experimental collapse moment. The reduced depth of the endplate (only 164 mm) involves a stress concentration in the contact zone. The compressive zone in the steel beam (displayed in dark) is quite bounded in height, thus the yielding cannot spread along the cross-section and the plastic resources of the beam are not optimally exploited. A tensile zone (displayed in bright)
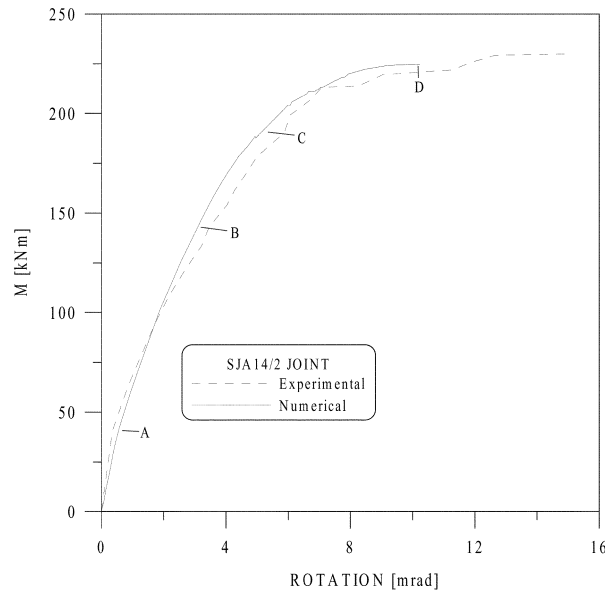
Fig. 14 Comparison between experimental and numerical results for the SJA14/2 joint in terms of moment vs. rotation curve

Table 6 Comparison between experimental and numerical moments for the SJA14/2 joint

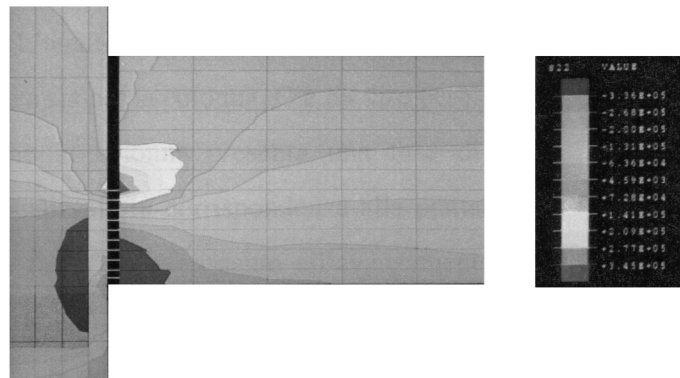| Values	Point A: first cracking	Point B: yielding of the column	Point C: yield. of the bars (X sect.)	Point D: yield. of the beam	Collapse
Experimental	47 (kNm)	140 (kNm)	197 (kNm)	228 (kNm)	236 (KNm)
Numerical	47 (kNm)	144 (KNm)	210 (KNm)	223 (KNm)	-

Fig. 15 Stress distribution in the column and steel beam for the SJA14/2 joint under 95% of the experimental collapse load (dark zones: compressive stresses; bright zones: tensile stresses; measures in kN/m^2)

can be recognized in the middle of the web. This zone is due to the upper bolts, which are subjected to tension and transmit this force to the endplate and to the beam web. The column shows a concentration of compressive stresses and plastic strains in the web panel near the bottom flange of the beam, because of the absence of web stiffening.
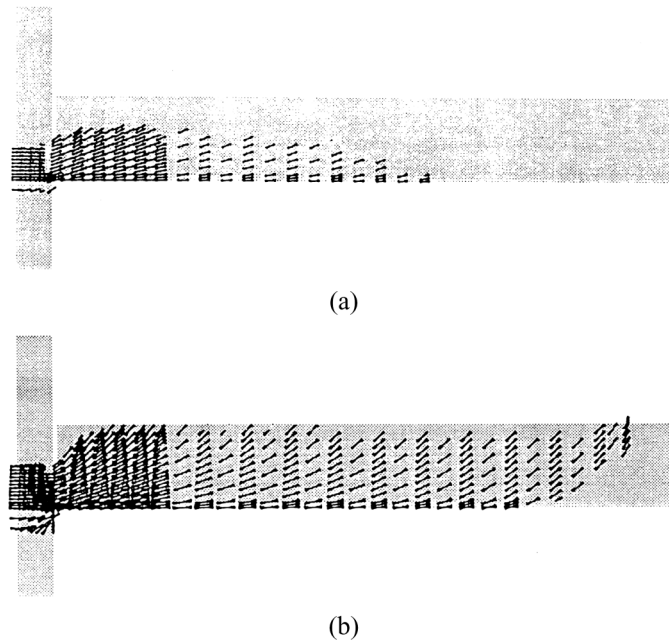
(a)

(b)

Fig. 16 Flux of compressive principal stresses in the column and steel beam for the SJA14/2 joint before the
concrete cracking (a) and near the collapse (b)

Fig. 16 provides a vectorial distribution of compressive principal stresses in the steel part of the
composite joint before the concrete cracking and near the collapse, respectively at 16% and 95% of the
experimental ultimate load. In the elastic phase, the compressive stresses flow from the steel beam to
the column mainly through the bottom flange of the beam. Near the collapse, the compressive stresses
flow mostly through the endplate, raising the neutral axis of the composite cross-section.

3.3. SJA14, SJA10, SJB14 and SJB10 semi-rigid joints

The numerical analyses discussed in this section refer to a series of experimental tests performed at
the University of Trieste in co-operation with the University of Trento (Benussi *et al.* 1989). The aim of
the tests was to investigate the influence of the type of reinforcement and steel beam-to-column
connection on the response of the composite joint. Four cruciform specimens characterised by two
different percentages of reinforcement and beam-to-column connections were tested.

The beam-to-column connections were realized by partial depth (SJA specimens, Fig. 17a) or flush
(SJB specimens, Fig. 17b) endplates welded, respectively, to the beam web and to both beam web and
flange. The endplates were bolted to the column flanges through four M20 Gr. 8.8 bolts. Column web
stiffening was obtained by horizontal steel plates aligned with the bottom flange of the beam. The
bottom reinforcement was made of eight 6 mm diameter bars. The top reinforcement was made of eight
14 mm diameter (joints type 14) or eight 10 mm diameter (joints type 10) bars, corresponding to a
medium (1.21%) or low (0.71%) percentage of reinforcement. The only difference between the joints
SJA14/2 and SJA14 is the presence of the column web stiffening in the latter.

The numerical modelling also fits well with the experimental responses in this case. The comparisons
for the joints SJA and SJB in terms of moment vs. rotation curves are reported in Figs. 18 and 19,
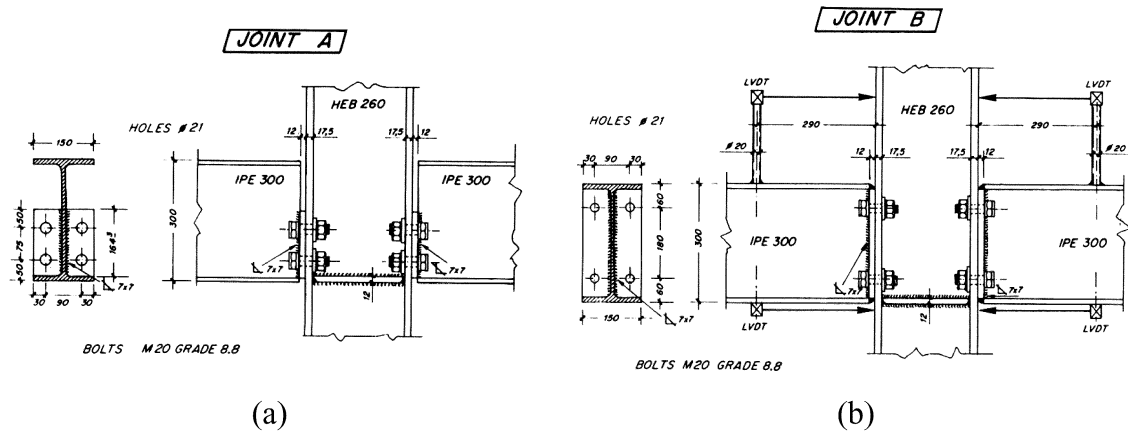
Fig. 17 Detail of the steel beam-to-column connection for the SJA (a) and SJB (b) joints
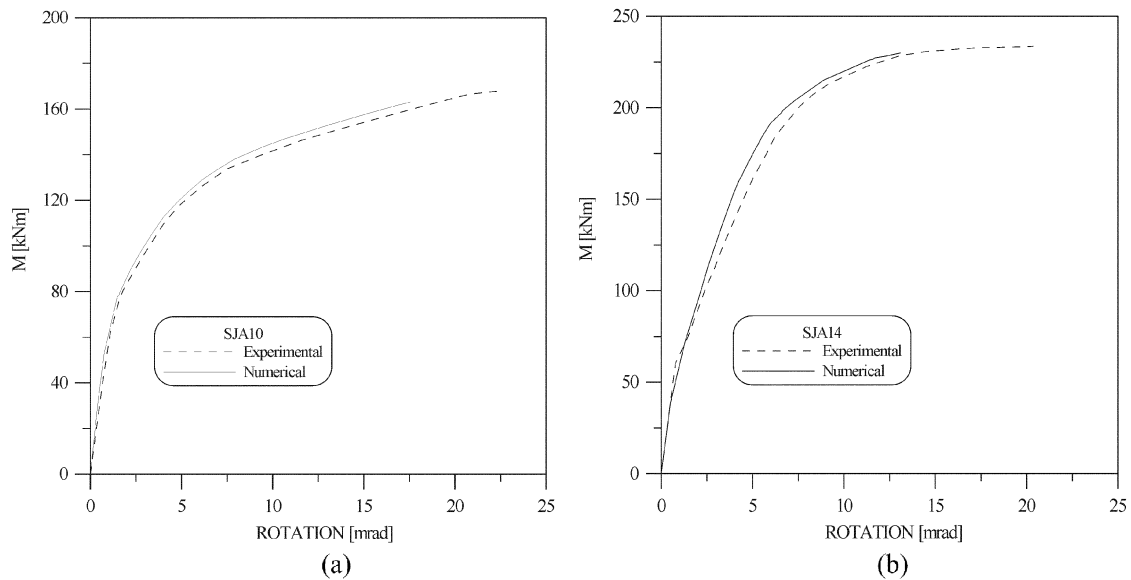

Fig. 18 Comparison between experimental and numerical results in terms of moment vs. rotation curve for the SJA10 (a) and SJA14 (b) joints

respectively. The experimental collapse load was not reached in any of the four numerical analyses because of convergence problems. However, the numerical collapse load was always larger than 95% of the experimental collapse load. This confirms the reliability of the adopted finite element modelling.

The semi-rigid joint SJB14 demonstrates behaviour similar to the rigid joint RJ14 in terms of both stiffness and strength, despite the rather simple details adopted. The main phenomena concerning the cracking of the concrete slab monitored during the test have been reproduced by the numerical analyses. The first crack appeared for values of the bending moment ranging between 12% and 16% of the collapse value. In all specimens, the cracks began at the most stressed part of the joint, i.e. at the end of the column flanges, and spread up to the slab edges at 20% of the ultimate moment, approximately corresponding to the cracking moment of the composite cross-section. The crack pattern did not depend
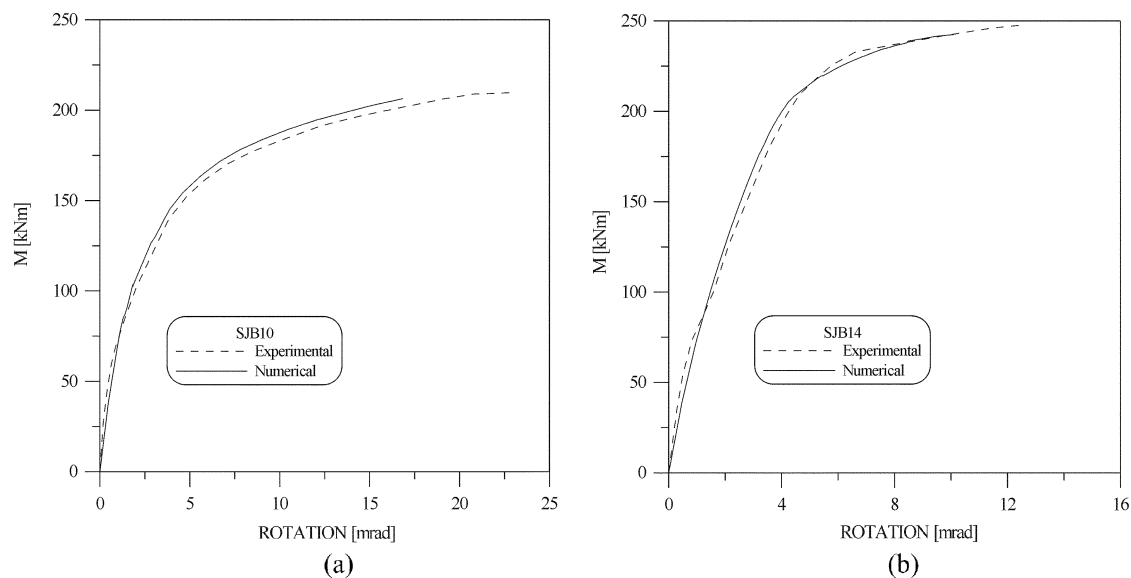
Fig. 19 Comparison between experimental and numerical results in terms of moment vs. rotation curves for the SJB10 (a) and SJB14 (b) joints

on the type of specimen and was characterised by a concentration of cracks in the zone of the slab weakened by the column profile.

4. Conclusions

The paper concerns a three-dimensional finite element modelling of rigid and semi-rigid steel-concrete composite joints under monotonic loading by using the Abaqus code. The aim of this study is to determine the strengths and shortcomings of this numerical approach.

A rigid joint and some different types of semi-rigid joints tested at the University of Trieste on cruciform specimens have been analysed. The load was applied statically and symmetrically on the specimens. The concrete slab and the steel parts (beam, column, endplates and web stiffening) have been modelled by using shell elements. An elastic-plastic with hardening law has been used for profile steel and reinforcement. A non-linear law with a softening branch in tension represents the behaviour of concrete. The connection between the slab and steel beam has been simulated by using concentrate spring elements with a non-linear shear vs. slip law. The contact between endplate and column flange has been modelled by fictitious beam elements with high compressive stiffness. The stress in these elements has been assessed at each loading step. If the stress turns to tension, the element is removed, according to a step-by-step updating procedure. Each bolt has been schematised through five non-linear beam elements parallel to the bolt axis loaded in such a way as to account for the preloading.

Through a comparison of numerical and experimental responses, the proposed finite element modelling is found to yield good results in terms of both global and local quantities, including moment vs. rotation curves, relative slips, cracking pattern, and stress distribution. Some convergence problems have arisen near the collapse; however the numerical ultimate load was larger than 95% of the

experimental collapse load in all cases. These problems make evaluation of the ultimate plastic rotation of the joint difficult, and experimental tests have thus far been the only reliable method in order to achieve this. The finite element modelling may represent the connecting link between experimental tests and mechanical and analytical modelling, allowing a better understanding of the experimental behaviour and detailed control of simplified approaches.

Owing to its complexity, this approach is not suitable for the practical design of composite joints, except for a few cases where simplified models cannot be used. In conclusion, the three-dimensional finite element modelling may be used to extend experimental results to other types of rigid and semi-rigid composite joints. The influence of different parameters, such as geometry and mechanical properties of materials, on the joint response can be investigated in detail. The calibration and validation of simplified mechanical or analytical models is another important issue that can be resolved by using this approach.

References

Amadio, C. and Altin, G. (1995), "Valutazione della risposta inelastica di travi composte acciaio-calcestruzzo mediante il codice di calcolo Abaqus", *Proc. of the 2nd Italian Workshop on Composite Structures*, Naples, Italy, June, 1-17 (in Italian).

Amadio, C. and Piva, M. (1995), "Valutazione della risposta di giunti composti rigidi o semi-rigidi mediante modellazione agli elementi finiti", *Proc. of the 15th C.T.A. Conf.*, Riva del Garda, Italy, October, 44-55 (in Italian).

Anderson, D. and Najafi, A.A. (1994), "Performance of composite connections: major axis end plate joints", *J. of Constructional Steel Research*, **31**(1), 31-57.

Aribert, J.M. (1995), "Influence of slip of the shear connection on composite joint behaviour", *Proc. of the 3rd Int. Workshop on Connections in Steel Structures*, Trento, Italy, May.

Bažant, Z. and Jirásek, M. (2002), *Inelastic Analysis of Structures*, John Wiley & Sons, LTD, Chichester, England.

Benussi, F., Nethercot, D.A. and Zandonini, R. (1995), "Experimental behaviour of semi-rigid connections in frames", *Proc. of the 3rd Int. Workshop on Connections in Steel Structures*, Trento, Italy, May.

Benussi, F., Puhali, R. and Zandonini, R. (1989), "Semi-rigid joints in steel-concrete composite frames", *Costruzioni metalliche*, **5**, 1-28.

Bursi, O.S. and Ballerini, M. (1997), "Low-cycle behaviour and analysis of steel-concrete composite substructures", *Proc. of the Int. Conf. on Composite Construction - Conventional and Innovative*, Innsbruck, Austria, September, 615-620.

Bursi, O.S. and Gramola, G. (1997), "Smeared crack analyses of steel-concrete composite substructures", *Proc. of the Stessa 97 Conf.,* Kyoto.

CEN, European Committee for Standardisation (1992), *Eurocode 3. Common Unified Rules for Steel Structure. ENV 1993-1-1.*

CEN, European Committee for Standardisation (1992), *Eurocode 4. Common Unified Rules for Composite Steel and Concrete Structures. ENV 1994-1-1.*

CEN, European Committee for Standardisation (1997), *Eurocode 4. Design of Composite Steel and Concrete Structures, Part 2. ENV 1994-2.*

Chen, W.F. (1984), *Plasticity in Reinforced Concrete*, McGraw-Hill, New York, U.S.A.

Comité Euro-International du Béton (1993), "CEB-FIP Model Code 90", *CEB Bull. No. 213/214*, Lausanne.

Comité Euro-International du Béton (1997), "Concrete Tension and Size Effects", *CEB Bull. No. 237*, Lausanne.

Crisfield, M.A. (1991), *Non-linear Finite Element Analysis of Solids and Structures. Vol. 1-2*, John Wiley & Sons Ltd., Chichester, England.

Cruz, P.J.S., Simões da Silva, L.A.P., Rodrigues, S.D. and Simões, R.A.D. (1998), "Database for the semi-rigid behaviour of beam-to column connections in seismic regions", *J. of Constructional Steel Research*, **46**(1-3), Paper No. 120.

Dissanayake, U.I., Burgess, I.W. and Davison, J.B. (2000), "Modelling of plane composite frames in unpropped

construction", *Eng. Struct.*, **22**(4), 287-303.

Faella, C., Piluso, V. and Rizzano, G. (2000), *Structural Steel Semirigid Connections*, CRC PRESS, Bola Raton, Florida, U.S.A.

Fang, L.X., Chan, S.L. and Wong, Y.L. (1999), "Strength analysis of semi-rigid steel-concrete composite frame", *J. of Constructional Steel Research*, **52**(3), 269-291.

Filippou, F. and Zulfiqar, N. (1992), "Model of critical regions and their effect on the seismic response of reinforced concrete frames", *Proc. of the 10th World Conf. on Earthquake Engineering,* Rotterdam, July.

Hibbit, Karlsson & Sorensen Inc. (1997), *Abaqus, Version 5.7*, U.S.A.

Kattner, M. and Crisinel, M. (2000), "Finite element modelling of semi-rigid composite joints", *Comput. Struct.*, **78**, 341-353.

Leon, R. (1990), "Semi-rigid composite construction", *J. of Constructional Steel Research*, **15**, 99-120.

Leon, R., Hoffmann, J. and Staeger, T. (1996), *Design of Partially Restrained Composite Connections*, AISC Design Guide 9, American Institute of Steel Construction, Chicago.

Leon, R. (1998), "Analysis and design problems for PR composite frames subjected to seismic loads", *Eng. Struct.*, **20**(4-6), 364-371.

Leon, R. and Darwin, D. (1998), "Design guide for partially restrained composite connections", *J. Struct. Eng.*, **124**(10), 1099-1114.

Leon, R., Hajjar, J., Gustafson, M. and Shield, C. (1998), "Seismic response of composite moment-resisting connections - II: behaviour", *J. Struct. Eng.*, **124**(8), 877-885.

Li, T.Q., Nethercot, D.A. and Choo, B.S. (1996a), "Behaviour of flush end-plate composite connections with unbalanced moment and variable shear/moment ratios-I. Experimental behaviour", *J. of Constructional Steel Research*, **38**(2), 125-164.

Li, T.Q., Nethercot, D.A. and Choo, B.S. (1996b), "Behaviour of flush end-plate composite connections with unbalanced moment and variable shear/moment ratios-II. Prediction of moment capacity", *J. of Constructional Steel Research*, **38**(2), 165-198.

Li, T.Q., Moore, D.B., Nethercot, D.A. and Choo, B.S. (1996c), "The experimental behaviour of a full-scale, semi-rigidly connected composite frame: overall considerations", *J. of Constructional Steel Research*, **39**(3), 167-191.

Li, T.Q., Moore, D.B., Nethercot, D.A. and Choo, B.S. (1996d), "The experimental behaviour of a full-scale, semi-rigidly connected composite frame: detailed appraisal", *J. of Constructional Steel Research*, **39**(3), 193-220.

Manfredi, G., Fabbrocino, G. and Cosenza, E. (1999), "Modeling of steel-concrete composite beams under negative bending", *J. Eng. Mech.*, **125**(6), 654-662.

Mazzolani, F.M. and Piluso, V. (1996), *Theory and Design of Seismic Resistant Steel Frames*, E & FN Spon, An Imprint of Chapman & Hall, London, U.K.

Nethercot, D.A. (1995a), "Design of composite connection", *The Structural Engineer*, **73**(13/4), 218-219.

Nethercot, D.A. (1995b), "Semi-rigid joint action and design of non-sway composite frame", *Eng. Struct.*, **17**(9), 554-567.

Nethercot, D.A. and Zandonini, R. (1989), *Methods of Prediction of Joint Behaviour: Beam-to-Column Connections. Stability and Strength*. Edited by R. Narayanan. Elsevier applied science, 23-62.

Nethercot, D.A. (1998), "Behaviour and design of composite connection", *Proc. of the Int. Conf. COST C1 "Control of the semi-rigid behaviour of civil engineering structural connections"*, Liège, September.

Puhali, R., Smotlak, I. and Zandonini, R. (1990), "Semi-rigid composite action: experimental analysis and a suitable model", *J. of Constructional Steel Research*, **15**, 121-151.

Ren, P., Crisinel, M. and Carretero, A. (1996), "Effets de la dalle en béton armé sur le comportement moment-rotation dassemblages métalliques pouter-poteau. Étude expérimentale, analyse numérique et méthode simplifiée", *Construction Métallique*, **3**, 3-24 (in French).

Stevens, N.J., Uzumeri, S.M., Collins, M.P. and Will, G.T. (1991), "Constitutive model for reinforced concrete finite element analysis", *ACI Struct. J.*, **88**(1), 49-59.

Tschemmernegg, F. and Queiroz, G. (1995), "Mechanical modelling of semi-rigid joints for the analysis of framed steel and composite structures", *Proc. of the 3rd Int. Workshop on Connections in Steel Structures*, Trento, Italy, May.

Tschemmernegg, F., Rubin, D. and Pavlov, A. (1998), "Application of the component method to composite joints", *Proc. of the Int. Conf. COST C1 "Control of the semi-rigid behaviour of civil engineering structural connections"*, Liège, September.

Wong, Y.L., Chan, S.L. and Nethercot, D.A. (1996), "A simplified design method for non-sway composite frames with semi-rigid connections", *The Structural Engineer*, **74**(2), 23-28.

Xiao, Y., Choo, B.S. and Nethercot, D.A. (1994), "Composite connections in steel and concrete. I. Experimental behaviour of composite beam-column connections", *J. of Constructional Steel Research*, **31**(1), 3-30.

Xiao, Y., Choo, B.S. and Nethercot, D.A. (1996), "Composite connections in steel and concrete. Part 2 Moment capacity of end plate beam to column connections", *J. of Constructional Steel Research*, **37**(1), 63-90.

Zandonini, R. (1989), *Semi-Rigid Composite Joints*. Edited by R. Narayanan. Elsevier applied science, 63-120.

DN